Two Classes of Alamethicin Transmembrane Channels: Molecular Models from Single-Channel Properties

Don-On Daniel Mak* and Watt W. Webb‡
*Physics Department, ‡School of Applied and Engineering Physics, Cornell University, Ithaca, New York 14853 USA

ABSTRACT Molecular structures of transmembrane channels formed by alamethicin polypeptide aggregates were analyzed by measuring open-channel conductances and state-transition kinetics using voltage-clamp technique with artificial phospholipid bilayers isolated onto micropipettes by a novel solvent-free tip-dip method. Two distinct classes of alamethicin channels, each with a unique set of conductance states and kinetic properties, were identified. Alamethicin R_f50 at low temperatures forms mostly nonpersistent channels with lifetimes of <1 min. Long-lasting persistent channels are formed by alamethicin R_f30 at all temperatures and by alamethicin R_f50 at room temperature. In the "modified barrel-stave" model for persistent channels based on the crystalline alamethicin secondary structure, the aqueous pore of the channel surrounded by parallel alamethicin monomers has a constriction generated by amino acid side chains protruding from the alamethicin helices into the pore. The model explains quantitatively the nonohmic channel conductance at high applied voltages and the conductance values and ion selectivities of various persistent channel states. The kinetic properties of nonpersistent channels are explained qualitatively by the "reversed-molecule" model in which nonpersistent channels differ from persistent channels by having one of the channel-forming alamethicin monomers oriented antiparallel to the others.

INTRODUCTION

Alamethicin is a 20-residue, antibiotic polypeptide (Rinehart et al., 1977; Balasubramanian et al., 1981) that forms voltage-dependent transmembrane channels (Mueller and Rudin, 1968). It has been intensely studied (for reviews, see Hall, 1978; Latorre and Alvarez, 1981; Sansom, 1991; Woolley and Wallace, 1992) because of its possible use as a model for more complex channels critical to the functioning of excitable membranes (Hall and Vodyanoy, 1984; Woolley and Wallace, 1992). Under an applied transmembrane potential of the correct polarity (Mueller and Rudin, 1968; Cherry et al., 1972), alamethicin readily forms well-defined channels with multiple conductance states (Gordon and Haydon, 1972) in a wide range of artificial lipid bilayers (Gordon and Haydon, 1976; Taylor and de Levie, 1991) and natural cell membranes (Sakmann and Boheim, 1979). The channels have long open durations (Boheim, 1974), especially in phospholipid bilayers at low temperatures (Gordon and Haydon, 1976). The size of a single alamethicin molecule is too small to form a conducting pore (Woolley and Wallace, 1992). This, together with the kinetics of alamethicin channel formation (Eisenberg et al., 1973; Gordon and Haydon, 1976; Hall and Vodyanoy, 1984), indicates that an alamethicin channel is an aggregate of a number of monomers. Individual alamethicin monomers in the channel aggregate have mainly helical conformations and span the lipid bilayer with the axes of the helices normal to the plane of the bilayer (Mathew and Balaram, 1983b; Spach et al., 1989). Channels are formed by bundles of such helices surrounding aqueous pores through which ions can pass across the lipid bilayer. However, because the conformations of individual alamethicin molecules and their arrangement inside the channel aggregate cannot be directly probed at present (Woolley and Wallace, 1992), the exact mechanisms underlying voltage-sensitive channel gating and transitions among conductance states are still controversial, with many conflicting models proposed (for reviews of the models, see Sansom, 1991; Woolley and Wallace, 1992). Furthermore, novel behavior of purified alamethicin under "reversed" applied voltage was reported (Taylor and de Levie, 1991). Therefore, despite the simple primary sequence of alamethicin and the extensive scrutiny of its characteristics in previous studies, the nature of the alamethicin channels and the mechanisms underlying its activities are far from being fully understood.

In our studies of single-channel currents in alamethicin channels using patch-clamp techniques (Hamill et al., 1981; Cahalan and Neher, 1992), we found that alamethicin polypeptides can form two classes of channels: alamethicin R_f50 at low temperatures (3–7°C) generates mostly *nonpersistent* channels that last a short time (<1 min), whereas the *persistent* channels that have a long lifetime (minutes to hours) are formed by alamethicin R_f30 at all temperatures and by alamethicin R_f50 at room temperature. Each class of alamethicin channels has a distinctive set of conductance states.

In this paper, we propose a "modified barrel-stave" model for persistent channels based on the crystalline secondary structure of the alamethicin molecules. This molecular model can quantitatively explain the nonohmic current-voltage relation for alamethicin channels at high applied voltage. By considering the conducting ions as "hard

Received for publication 6 February 1995 and in final form 7 September 1995.

Address reprint requests to Dr. Don-On Daniel Mak, Department of Physiology, University of Pennsylvania, Stellar-Chance Laboratories, Rm. 313B, 422 Curie Blvd., Philadelphia, PA19104-6069 USA Tel.: 215-898-0468; Fax: 215-573-8590.

0006-3495/95/12/2323/14 $2.00

spheres" with a finite radius, the conductance values and ion selectivities of the various persistent channel conductance states can be deduced from the molecular model. We also propose a "reversed-molecule" model in which the nonpersistent channels differ from the persistent channels by having one of the channel-forming alamethicin monomers oriented antiparallel to the others. This model qualitatively explains the existence, the relative abundance at various temperatures, and the kinetic properties of the nonpersistent channels. Our molecular models support the mechanisms proposed by Baumann and Mueller (1974) for voltage-dependent gating and conductance state transition in alamethicin channels.

MATERIALS AND METHODS

Materials

Alamethicin was either purchased from Sigma Chemical Co. (St. Louis, MO) or received as a gift from Upjohn Co. (Kalamazoo, MI). Alamethicin from Sigma was purified by high-performance liquid chromatography (HPLC) following the procedures used by Balasubramanian et al. (1981). A HPLC chromatogram with eight well-resolved mass peaks very similar to that in Balasubramanian et al. (1981) was obtained. Only the most abundant component, which is at least twice as abundant as any other component, was isolated for use as purified alamethicin in our experiments. No impurity mass peak was resolved by HPLC in the purified sample. Mass spectrometry (Archer et al., 1991) showed this to be alamethicin R_f50 with the primary sequence: Ac-Aib-Pro-Aib-Ala-Aib^5-Ala-Gln-Aib-Val-Aib^{10}-Gly-Leu-Aib-Pro-Val^{15}-Aib-Aib-Gln-Gln-Phol^{20} where Aib and Phol stand for α-aminoisobuteric acid and L-phenylalaninol respectively. It exists as electrically neutral molecules in aqueous solution at pH 7 (Rizzo et al., 1987; Stankowski et al., 1988). Alamethicin from Upjohn was used without further purification. Its major component is alamethicin R_f30 (Martin and Williams, 1975; Balasubramanian et al., 1981) with Glu in position 18, which carries a negative charge at pH 7 (Gisin et al., 1977). It also contains other minor components with slightly different primary sequences (Rinehart et al., 1977; Marshall and Balasubramanian, 1979).

Azolectin from Sigma Chemical Co., synthetic dioleoyl phosphatidylethanolamine (DOPE) and dioleoyl phosphatidylserine (DOPS) from Avanti Polar Lipids, Inc. (Alabaster, AL), and cholesterol from Nu Chek Prep Inc. (Elysian, MN) were used to produce lipid bilayer without further purification.

Solvent-free tip-dip technique

The tip-dip method had been developed to isolate phospholipid bilayers onto the tips of micropipettes (Coronado and Latorre, 1983) in patch-clamp experiments (Hamill et al., 1981). However, to avoid any artifact that may be caused by residual traces of the organic solvent used to spread the lipid monolayer on the buffer/air interface, a truly solvent-free tip-dip procedure similar to that used by Hanke et al. (1984) was adopted. Synthetic DOPE and DOPS in chloroform were mixed in 1:1 molar ratio with various amounts of cholesterol. The lipid solution was dried under vacuum overnight. The same buffer solution used in the patch-clamp experiment was added to the dried lipid (0.025 ml/mg of lipid). The mixture was vortexed briefly and sonicated in an ice bath for 15 min. The resulting cloudy lipid suspension showed no visible vesicles under 100× magnification. The sonication dispersed the lipid in the buffer, enabling the formation of the lipid monolayer at the buffer/air interface without the use of organic spreading solvent. Suspension of azolectin in buffer solution was also prepared in the same manner. The lipid suspensions were stored in liquid nitrogen. They were thawed just before the experiment and diluted to a concentration of 4 mg of lipid/ml with more buffer solution. Lipid suspension (25–50 μl) was added to 5 ml of bath buffer solution containing 5 mM $CaCl_2$, 1 mM $MgCl_2$ (Coronado, 1985), and 30 mM HEPES at pH 7 with variable NaCl concentration between 0.33 and 2.0 M. Fifteen to thirty minutes was allowed for a lipid monolayer to form over the buffer/air interface. The tip of a buffer-filled, heat-polished pipette was moved through the interface several times until a lipid bilayer formed over the tip of the pipette, indicated by an abrupt increase in the pipette resistance. A negative pressure of about 20 mm Hg was applied inside the pipette to improve the seal (Hamill et al., 1981). This procedure generated stable seals of about 2–20 GΩ in over 80% of all attempts using DOPE/DOPS mixtures. A similar procedure using azolectin generated seals with 20–40 GΩ resistance.

Single-channel current measurement and analysis

Single-channel alamethicin current records with characteristic multiple conductance states were obtained with 0.02–1.00 μg/ml alamethicin on the pipette side or both sides of the bilayer. The appropriate amount of alamethicin for single-channel recording depended on the buffer ionic concentration and the lipid bilayer composition.

By cooling the bath buffer solution in experiments to 7.0 ± 0.2 °C with a Peltier cooling stage (OPMI-2; Medical Systems Corp., Greenvale, NY), the frequency of transitions among alamethicin channel conductance states was decreased (Boheim, 1974; Gordon and Haydon, 1976; Boheim and Kolb, 1978) to facilitate open-channel current noise measurement.

Single-channel currents were amplified by a patch-clamp amplifier (3900A with headstage 3901; Dagan Corp., Minneapolis, MN); filtered at 37 kHz by a 4-pole Bessel filter; digitized at 94.4 kHz by a pulse code modulator (VR-10; Instrutech Corp., Mineola, NY); and recorded with 14-bit resolution on videotape. Manually selected records were transferred to a Convex mini-supercomputer for analysis.

A computer program was written to monitor the average and standard deviation values of current data points in consecutive 1.36-ms periods. A conductance state transition was detected if either of the monitored values fluctuated by more than 1.3 times their normal ranges. In simulated current records, brief changes in conductance state lasting longer than 0.04 ms were detected by the program. With the time between the entry of the channel into any conductance state and its subsequent departure determined, the average dwell time of conductance state n can be calculated as the total duration the channel spent in state n in the experiment divided by the number of state $n \rightarrow (n \pm 1)$ transitions detected during the experiment.

In every selected current record with a stable lipid bilayer, the current level for each conductance state stayed within a very narrow range throughout the experiment, independent of the number of conductance state transitions that occurred. Thus, the mean current level $\langle i_n \rangle$ averaged over all the time when the channel was in state n is well defined. The 0th (closed) state mean current level $\langle i_0 \rangle$ was the same as that of the bare bilayer leakage current before the channel appeared. This background current was subtracted from the mean current levels of the open-channel states to obtain the current actually passing through the channel $i_n^{ch} = \langle i_n \rangle - \langle i_0 \rangle$.

RESULTS

Channels from purified alamethicin R_f50

Two distinct sets of conductance states were observed for channels formed by HPLC-purified alamethicin R_f50. In some cases, the alamethicin channel appeared readily when a positive potential (usually >25 mV) was applied on the side of the bilayer where alamethicin was present after the gigaohm seal was formed. The channel stayed open for a long period of time (minutes, even hours) and only closed very briefly and infrequently. Fig. 1 shows a typical current record of this class of persistent channel.

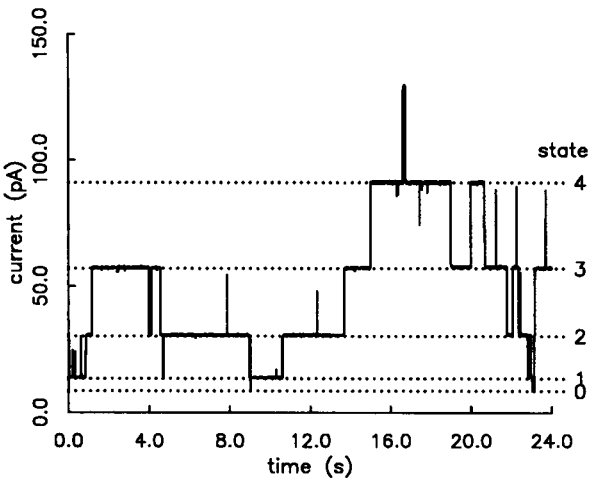

FIGURE 1 A typical current record of a persistent channel formed by purified alamethicin R_f50. The buffer solution contained 1.0 M NaCl. The lipid bilayer was formed by DOPE and DOPS mixture in 1:1 ratio. Only the pipette buffer contained 0.2 μg/ml alamethicin. Temperature of the bath buffer was 7.0°C. Applied potential for this record was +44 mV. The record has been digitally filtered at 737.5 Hz for plotting purposes.

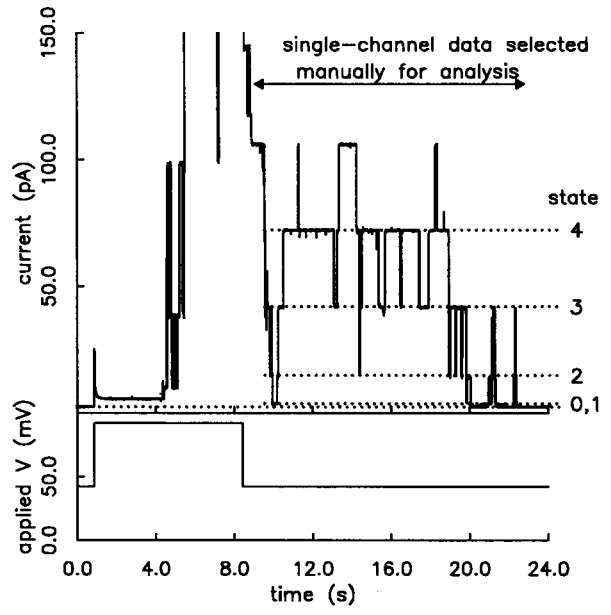

FIGURE 2 A typical current record of a nonpersistent channel formed by purified alamethicin R_f50. The same experimental conditions and digital filtering were used in Fig. 1. The holding potential during the single-channel data was +42 mV. The channel-inducing pulse went up to 92 mV.

In contrast, in most trials (over 95% of all experiments), channels had to be induced by applying a potential higher than a critical value (90–150 mV, depending on the concentration of alamethicin in the buffer solution). Once channels appeared, multiple channels rapidly formed in the bilayer under the high applied potential. The applied potential then had to be lowered to a holding value (30–80 mV) to obtain single-channel current records. The channel stayed open for a relatively short period of time (0.5–80.0 s) before it closed completely. Fig. 2 shows a typical current record for this class of nonpersistent channel. The channel shown closed completely after t = 22.5 s. Once the channel closed completely, no channel would reappear if the applied potential was kept at the holding value. Another pulse of applied potential higher than the critical value was needed to re-induce another channel opening.

Both persistent and nonpersistent channels were observed in a wide range of experimental conditions. Both were observed in buffer solution with NaCl concentrations of 0.33, 1.0, and 2.0 M; in bilayers made with azolectin, DOPE:DOPS = 1:1 mixture and DOPE:DOPS:cholesterol = 2:2:1 mixture; with alamethicin present on one side or both sides of the bilayer. Nonpersistent channels were always predominantly observed. In some experiments, two channels were observed in the bilayer simultaneously, one being persistent and the other nonpersistent. However, conversion of persistent to nonpersistent channels or vice versa without the channel closing was rarely observed.

Within the range of applied potential used (between −68 mV and +80 mV), the mean channel current i_n^{ch} in each conductance state of both persistent and nonpersistent channels was directly proportional to the applied potential V_{ap} (Fig. 3). The conductance values Λ_n of the persistent and nonpersistent channels at various conductance states were calculated from the slope of the graphs: $\Lambda_n = i_n^{ch}/V_{ap}$. The conductance values of the persistent channel states were consistently higher than those of the corresponding nonpersistent channel states.

Despite the wide range of the average dwell times for the persistent and nonpersistent channels under various experimental conditions, the average dwell time a persistent channel spent in conductance state n was generally much longer than that of a nonpersistent channel under similar experimental conditions (Table 1), especially for lower conductance states.

Channels from unpurified alamethicin R_f30

When unpurified alamethicin from Upjohn Co. was used in our patch-clamp experiments, nonpersistent channels were not observed. Channels remained active for minutes and closed only for brief intervals (Fig. 4). Besides the regular set of "normal" conductance states n, for about 15% of the time the channels occupied another set of "odd" conductance states n', each with a conductance value smaller than the corresponding normal state n. The current levels of both the normal and odd conductance states were stable and ohmic between 20 and 80 mV. Careful examination of the current records showed that the majority of conductance state transitions involve normal states only (state $n \rightarrow$ state $(n \pm 1)$) or odd states only (state $n' \rightarrow$ state $(n \pm 1)'$). Whereas transitions involving both normal and odd states ($n \rightarrow (n+1)'$ and $n' \rightarrow (n-1)$) were also observed, other combinations ($n \rightarrow (n-1)'$, $n' \rightarrow (n+1)$, $n \rightarrow n'$, and $n' \rightarrow n$) were not observed. In experiments done by Taylor

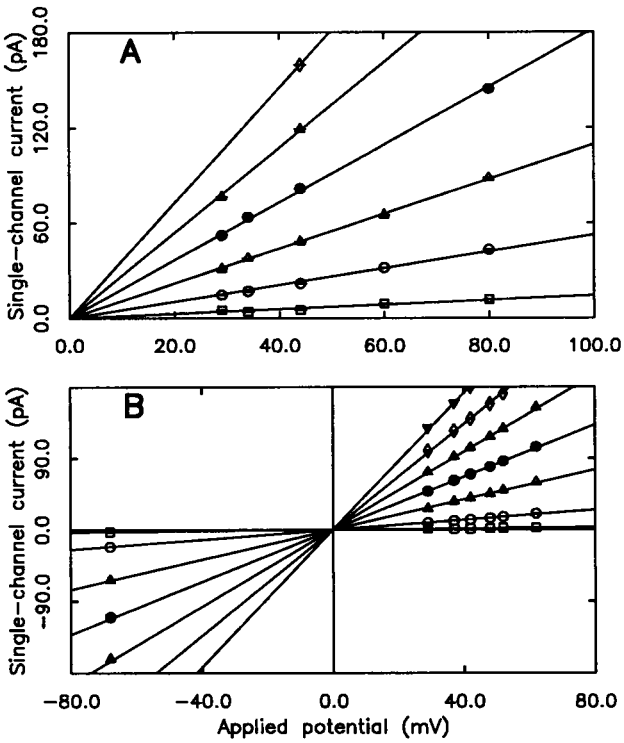

FIGURE 3 Graphs of single-channel current versus applied potential for various conductance states of a persistent channel (*A*) and a nonpersistent channel (*B*). The same experimental conditions were used in Fig. 1. Current measurement under negative applied potential was rarely successful because of the low probability of forming alamethicin channels under negative applied potential (Eisenberg et al., 1973)

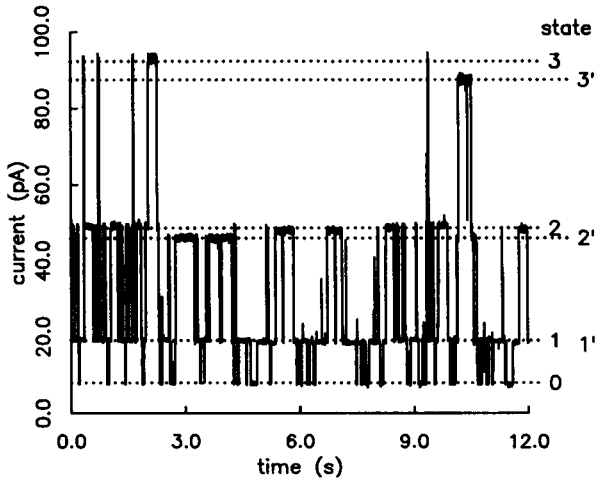

FIGURE 4 A current record of a channel formed using unpurified alamethicin R_f30 with normal states n and odd states n' in the same buffer solution as in Fig. 1. The lipid bilayer was formed by azolectin. The pipette buffer solution contained 0.02 μg/ml alamethicin. Temperature of the bath buffer solution was 23°C. Applied potential was 60 mV. The record was digitally filtered at 737.5 Hz.

and de Levie (1991) using HPLC-purified alamethicin R_f30 from Upjohn Co. under very similar conditions (in diphytanoylphosphatidylcholine and cholesterol (2:1) bilayer in 0.5 M KCl at 19°C), only one set of conductance states was reported.

The properties of the odd conductance states can be understood using the standard "barrel-stave" model (Baumann and Mueller, 1974) in which the channel changes its conductance state when a single alamethicin molecule joins or leaves the channel-forming aggregate. The channels

TABLE 1 Average dwell time (s) of the various conductance states of alamethicin channels

	Our experiment data* applied potential = 44 mV		Previous data‡ applied potential = 90 mV	
State	Persistent	Nonpersistent	R_f30	R_f50
1	0.21	0.022	0.259	0.0305
2	0.52	0.026	0.341	0.0361
3	0.74	0.11	0.405	0.0664
4	0.33	0.16	0.556	0.110
5	0.11	0.10	0.575	0.124
6	0.10	0.06	—	—

*Data from our experiments (±0.002 s) using purified alamethicin R_f50 in DOPE/DOPS bilayer in 1 M NaCl at 7°C.

‡Data obtained by Boheim (1974) using purified alamethicin R_f30 and R_f50 in PS bilayer in 1.0 M KCl at 3°C.

in normal conductance states observed most of the time are entirely formed by molecules of alamethicin R_f30, the major component in unpurified Upjohn samples. A channel in an odd state n' probably contains a single molecule of some minor alamethicin component, resulting in a channel configuration with a smaller pore. This is similar to the formation of "hybrid" channels with conductance values different from those of pure alamethicin channels in mixtures of alamethicin R_f30 and its dansyl derivative (Eisenberg et al., 1977). In this model, a channel in a normal state can only enter an odd state if the channel is joined by a non-R_f30 molecule, resulting in an $n \rightarrow (n + 1)'$ transition. The channel will remain in the odd states with $n' \rightarrow (n \pm 1)'$ transitions as long as the non-R_f30 molecule remains in the channel while other alamethicin R_f30 molecules join or leave the channel aggregate. The channel only returns to a normal state when the non-R_f30 molecule leaves the channel in an $n' \rightarrow (n - 1)$ transition. Those transitions ($n \rightarrow n'$, $n' \rightarrow n$, $n \rightarrow (n - 1)'$ and $n' \rightarrow (n + 1)$) that cannot be achieved by a single alamethicin molecule (R_f30 or non-R_f30) joining or leaving the channel were not observed.

Because normal states occurred about 85% of the time and there are five to seven alamethicin molecules in the first few conductance states, the probability that the molecule joining a channel is a R_f30 molecule ≈ 0.97, according to simple binomial distribution. Because alamethicin R_f30 only makes up about 45% of the unpurified Upjohn samples (Balasubramanian et al., 1981), R_f30 molecules must have a higher affinity than other non-R_f30 molecules to join a channel. The probability of forming a channel with two non-R_f30 molecules ≈ 0.01, too low to be clearly observed in our experiments.

Comparison with previous studies

Comparison of electrical and kinetic properties of alamethicin channels formed by a single alamethicin species observed in our experiments with those previously reported reveals that whereas pure alamethicin R_f50 at low temperatures (3–7°C) forms mostly (>95%) nonpersistent channels, persistent channels are formed by alamethicin R_f50 at room temperature and by alamethicin R_f30 at all temperatures.

Although various kinetic and electrical properties of single alamethicin channels have been investigated in many previous experiments (Gordon and Haydon, 1972, 1976; Eisenberg et al., 1973; Boheim, 1974; Hall, 1975; Bezrukov and Vodyanoy, 1993), no systematic, quantitative comparison of the results of those studies has been done because of the wide range of different conditions (temperature, bilayer lipid and buffer ion compositions) used in various experiments. Assuming that alamethicin channel conductance is directly proportional to the buffer solution conductivity (Eisenberg et al., 1973, 1977), corrected channel conductance values under a standard set of conditions (in 1.0 M NaCl at 7.0°C, our experimental conditions) were calculated from experimental conductance values using electrolyte conductivity data from Washburn (1929). All published numerical conductance values of alamethicin channels (Eisenberg et al., 1973; Boheim, 1974; Bezrukov and Vodyanoy, 1993) are included in our comparison.

The conductance values of normal channel states we obtained with unpurified Upjohn alamethicin (*E* in Fig. 5) agree with the corrected values measured by Eisenberg et al. (1973), also using unpurified Upjohn alamethicin (*D* in Fig. 5), and those measured by Boheim (1974) with purified alamethicin R_f30 (*C* in Fig. 5). This shows that the corrected conductance values reflect the nature of the channel and are independent of the environment around the channel. It also confirms that channels with normal conductance states observed in our experiments using unpurified Upjohn alamethicin were formed entirely by alamethicin R_f30 molecules. However, no odd states were reported by Eisenberg et al. (1973).

These conductance values obtained for alamethicin R_f30, purified or unpurified, agree with those of the rare persistent channels obtained in our experiments (*B* in Fig. 5) and those measured by Bezrukov and Vodyanoy (1993) (*A* in Fig. 5), both using purified alamethicin R_f50. Thus, pure alamethicin R_f50 molecules can form channels with the same conductance values as those formed by pure alamethicin R_f30 molecules, so the conductance of channels is not entirely determined by the primary sequence of the alamethicin molecules.

The conductance values of the nonpersistent channels obtained in our experiments with purified alamethicin R_f50 at 7°C (*G* in Fig. 5) agree with those obtained by Boheim (1974) for purified alamethicin R_f50 (*H* in Fig. 5) under similar temperature. The requirement of an inducing potential pulse to generate the nonpersistent channels in our experiments was not reported by Boheim (1974). Such differences in channel kinetic behavior can be due to differences in experimental conditions and protocols used (Boheim, 1974). Bezrukov and Vodyanoy (1993) only reported observing persistent channels when using purified alamethicin R_f50 at room temperature. Apparently the relative frequency of observing the persistent and nonpersistent channels is strongly affected by temperature, with nonpersistent channels dominating under low temperatures and persistent channels dominating at room temperature.

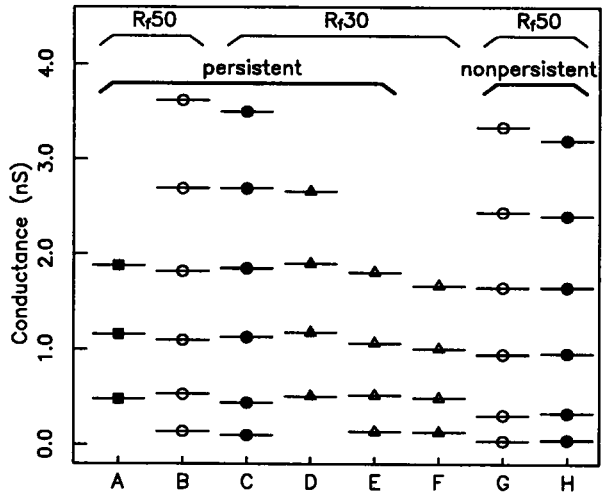

FIGURE 5 Conductance values of various conductance states of alamethicin channels obtained in our experiments (*open symbols*) and previously reported (*filled symbols*). All conductance values plotted are measured in or corrected to buffer conditions of 1.0 M NaCl at 7°C. Open circles are experimental conductances from our experiments of persistent (*B*) and nonpersistent (*G*) channels formed by purified alamethicin R_f50 in DOPE/DOPS bilayer in 1.0 M NaCl at 7°C. Open triangles are corrected conductances from our experiments for normal (*E*) and odd (*F*) conductance states formed by unpurified alamethicin in azolectin bilayer in 1.0 M NaCl at 23°C. Filled circles are the corrected conductances of channels formed by purified alamethicin R_f30 (*C*) and R_f50 (*H*) in PS bilayer as measured by Boheim (1974) in 1.0 M KCl at 3°C. Filled triangles (*D*) are the corrected conductances of channels formed by unpurified alamethicin in PE bilayer as measured by Eisenberg et al. (1973) in 2.0 M NaCl at 23°C. Filled boxes (*A*) are the corrected conductances of channels formed by purified alamethicin R_f50 in diphytanoyl PC bilayer as measured by Bezrukov and Vodyanoy (1993) in 1.0 M NaCl at 23°C.

Whereas the conductance values of odd states formed with unpurified samples (*F* in Fig. 5) are ≈94% of those for the corresponding normal states (*E* in Fig. 5), those of nonpersistent channels formed by purified alamethicin R_f50 (*G* in Fig. 5) do not have any simple relation with the persistent channel values (*B* in Fig. 5). Besides, transitions between normal and odd states were observed much more frequently than transitions between persistent and nonpersistent channels. Therefore, nonpersistent channels are fundamentally different from odd conductance states caused by impurity molecules in the channel aggregate.

Besides the conductance values, mean dwell times of the channel in various conductance states (or rates of conductance state transitions) were also widely reported (Boheim, 1974; Gordon and Haydon, 1975, 1976). However, there is

no simple relation describing the large effects of temperature, applied potential, buffer ion, and bilayer lipid compositions on alamethicin channel dwell times in various conductance states (Boheim, 1974; Gordon and Haydon, 1976; Boheim et al., 1983; Hall and Vodyanoy, 1984). Therefore, we can only compare channel dwell times we observed with those obtained by Boheim (1974) under similar experimental conditions (at 3°C using PS bilayer in 1 M KCl buffer). The dwell times of the various persistent channel conductance states in our experiments agree reasonably well with those of alamethicin R_f30 channels observed by Boheim (1974) (Table 1), whereas those of nonpersistent channel states are similar to those of alamethicin R_f50 channels observed by Boheim (1974). This further supports our conclusion that the alamethicin R_f50 channels observed by Boheim (1974) are our nonpersistent channels; and the persistent channels we formed with purified alamethicin R_f50 are those that were previously only observed in alamethicin R_f30 samples.

DISCUSSION

Nonohmic behavior of channel current

The relation between alamethicin channel current i_n^{ch} in various conductance states n and the applied potential V_{ap} was investigated previously (Eisenberg et al., 1973; Gordon and Haydon, 1975; Taylor and de Levie, 1991) over a wide range of V_{ap}. Although i_n^{ch} was found in many experiments (Eisenberg et al., 1973, 1977; Boheim, 1974) to be proportional to V_{ap} for $|V_{ap}| < 100$ mV, which agrees with our experimental results (Fig. 3), the relation is super-linear for alamethicin channels in phospholipids under $|V_{ap}| > 100$ mV (Eisenberg et al., 1973; Taylor and de Levie, 1991). This nonohmic relation between i_n^{ch} and V_{ap} can be explained using a model proposed by Laüger (1975) in which the channel current i_n^{ch} was regarded as bidirectional, thermally activated transport of ions over a single energy barrier inside the channel, like the movement of electrons in a saturated thermionic diode. Thus, in an experiment with equal concentration $\bar{\rho}$ of monovalent ions on both sides of the membrane,

$$i_n^{ch} = e_o A_n \bar{\rho}\left(\frac{kT}{h}\right)\left[2\sinh\left(\frac{e_o V_{ch}}{2kT}\right)\right] \times \left[\exp\left(\frac{-E_n^+}{kT}\right) + \exp\left(\frac{-E_n^-}{kT}\right)\right], \quad (1)$$

where k is Boltzmann's constant, T the temperature of the system, h Planck's constant, and e_o the electron charge. The proportionality constant A_n factors in the channel pore size. The potential drop across the channel is V_{ch}. The energy barrier terms, E_n^+ for cations and E_n^- for anions, determine the ion selectivity of the channel. The model is applicable as long as the ions experience only one prominent energy barrier during transport through the channel. No details concerning the form of the potential barrier inside the channel or dimensions of the channel have to be assumed. The channel current according to this model is proportional to $\sinh(e_o V_{ch}/2kT)$ and therefore is proportional to V_{ch} for $e_o V_{ch} \ll 2kT$ and changes more steeply for larger V_{ch}, as observed by Eisenberg et al. (1973) and Taylor and de Levie (1991).

In series with this nonohmic resistance R_n^{ch} of the channel itself is an ohmic spreading or access resistance R_n^{sp} caused by the high current density in the vicinity of the channel (Holm, 1967). Thus, the actual potential drop across the channel V_{ch} is only a fraction of the applied potential V_{ap} across the lipid bilayer: $V_{ch} = c_n V_{ap}$, where c_n (<1) is a constant with a unique value for each conductance state n. From Eq. 1,

$$i_n^{ch} \propto \sinh\left(\frac{e_o c_n V_{ap}}{2kT}\right). \quad (2)$$

Values for c_n (Table 2) were derived by fitting Eq. 2 to the experimental data from Taylor and de Levie (1991) (Fig. 6). From the values of c_n, the magnitude of the spreading resistance around the alamethicin channel $R_n^{sp} = (1 - c_n)/\Lambda_n$ can be calculated.

Because the persistent channel is enclosed by a bundle of identical alamethicin molecules (Mathew and Balaram, 1983b; Spach et al., 1989), the channel pore must be highly symmetric. We represent the channel pore with a circular pore, the only configuration with an analytical formula for its spreading resistance (Maxwell, 1873; Smythe, 1967; Hille, 1984a). We define the equivalent radius r_n^{eq} of a channel in conductance state n as the radius of the circular pore with the same spreading resistance as the channel,

$$r_n^{eq} = \left(\frac{\Lambda_n}{1 - c_n}\right)\left(\frac{1}{2\sigma}\right), \quad (3)$$

where σ is the conductivity of the buffer solution. The values of r_n^{eq} calculated (Table 2) are significantly smaller than those channel radii previously calculated using simple models of alamethicin channels, assuming that the channel pore has a uniform cross section throughout its length (Boheim, 1974; Baumann and Mueller, 1974; Hanke and Boheim, 1980; Sansom, 1991). The r_n^{eq} for the first conductance state is smaller than the ionic radius of Na^+ (Hille,

TABLE 2 Channel parameters for various conductance states of alamethicin channels

	Persistent channel			Nonpersistent channel	
State	c_n	r_n^{eq} (Å)	r_n^{max} (Å)	r_n^{eq} (Å)	r_n^{max} (Å)
1	0.80	0.60	1.57	0.29	1.51
2	0.61	1.15	2.25	0.91	2.20
3	0.49	1.84	2.94	1.80	2.90
4	0.42	2.68	3.63	2.61	3.61
5	0.37	3.64	4.33	3.44	4.33
6	0.325	4.58	5.04	4.33	5.04
7	—	—	—	5.26	5.76

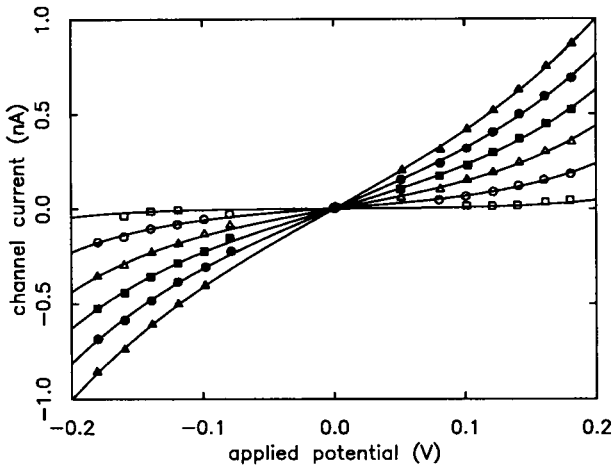

FIGURE 6 Graph of experimental persistent channel current versus voltage applied across the lipid bilayer for various conductance states. The points are data obtained by Taylor and de Levie (1991) from persistent channels formed by purified alamethicin R_f30 in diphytanoylphosphatidylcholine and cholesterol (2:1) bilayer in 0.5 M KCl at 19°C. The lines are fitted using Eq. 2 and values of c_n in Table 2.

1984b). To understand this, we propose a modified "barrel-stave" model for the channel.

Modified "barrel-stave" model for persistent channels

The original barrel-stave model (Baumann and Mueller, 1974), in which the alamethicin channels in various conductance states contain different numbers of monomers in the channel-forming aggregate and conductance state transitions occur when an alamethicin monomer joins or leaves a channel aggregate, still explains most satisfactorily, among various proposed models, the large number of distinct conductance states observed (Gordon and Haydon, 1975; Fleischmann et al., 1983). However, previous efforts in quantitatively explaining the observed channel conductance values from molecular models were too simplistic. Contribution of the spreading resistance to the channel resistance was ignored in most of them. Also, extremely simple three-dimensional geometric forms were assumed for alamethicin molecules in the channels. The planar form proposed (Baumann and Meuller, 1974; Mueller, 1976; Hanke and Boheim, 1980) ignored the volume occupied by the alamethicin molecules so that the pore size is overestimated (Mathew and Balaram, 1983a). The cylindrical form (Sansom, 1991; Lavar, 1994) was very different from the actual shape of the alamethicin molecules, with amino acid side chains of different shapes and sizes protruding from the helix. For a better model of the alamethicin channel, we assume a more realistic shape for the alamethicin molecule based on its experimentally determined secondary structure.

Although the secondary structures of alamethicin, its fragments, and analogues have been extensively studied in bilayers, vesicles, and various solvents by a wide range of techniques including x-ray diffraction (Butters et al., 1981; Fox and Richards, 1982; Bosch et al., 1985), nuclear magnetic resonance (Davis and Gisin, 1981; Banerjee et al., 1983; Schmitt and Jung, 1985; Esposito et al., 1987; Chandrasekhar et al., 1988; Yee and O'Neil, 1992; Kelsh et al., 1992), circular dichroism (Vogel, 1987; Cascio and Wallace, 1988), Raman spectroscopy (Vogel, 1987), theoretical molecular dynamics simulation (Fraternali, 1990), and energy optimization (Furois-Corbin and Pullman, 1988; North et al., 1994) (for review, see Sansom, 1991, 1993), the precise conformation of alamethicin molecules inside the special environment of a channel has not been determined by experiment (Woolley and Wallace, 1992). Experimental evidence indicated that because of the large number of α-aminoisobuteric acid (Aib) residues present in the alamethicin molecule, its conformation is largely helical (Burgess and Leach, 1973; Paterson et al., 1981; Marshall et al., 1990) and very stable (Jung and Dubischar, 1975; Esposito et al., 1987). In the hydrophobic environment of a lipid bilayer, the secondary structure is more ordered (Vogel, 1987; Cascio and Wallace, 1988) and helical (Haris and Chapman, 1988) than in organic solvents, especially in the presence of a transmembrane electric field of the right polarity (Brumfeld and Miller, 1989). Furthermore, the distribution of residues in the crystalline conformation described by Fox and Richards (1982) generates an amphipathic structure (Kerr and Sansom, 1993) that will be stabilized at the water-lipid interface inside the channel, with the polar elements facing the aqueous channel pore. Therefore, for our modeling purpose, we assume the highly helical structure described by Fox and Richards (1982) as an approximation for the conformation of the alamethicin molecules forming the channel.

Besides the conformation of the alamethicin molecules forming the channel, the conductance of the channel is also determined by the arrangement of alamethicin helices around the channel pore. In a channel configuration proposed by Fox and Richards (1982), the N-terminal helices of the molecules are roughly parallel to the channel axis, so that the channel has a funnel shape, with a wider channel pore at the C-terminals of the alamethicin molecules. The relatively large side chain of the phenylalaninol will help to fill the interhelical free volume at the wider end of the channel (Vogel et al., 1993). The side chains of Gln^7 protrude into the channel pore in a plane that is normal to the channel axis, forming a constriction in the channel pore (Fig. 7 *A*). Energy calculations by Sansom (1993) indicated that this molecular arrangement is stable and can form channels containing variable numbers of molecules (as required by the barrel-stave model). In this configuration, the Glu^{18} side chains are far from the channel pore, so the model agrees with the experimental finding that binding a methyl ester (Eisenberg et al., 1977; Hall, 1978) or benzyl ester (Boheim et al., 1987) to the carboxyl group of the Glu^{18} of alamethicin R_f30 did not affect the conductance of the alamethicin R_f30 channels. Using that model, we assume that the resistance of the channel itself R_n^{ch} is mostly

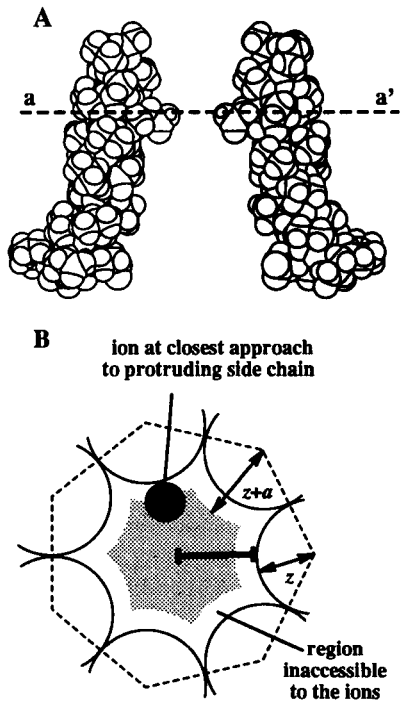

FIGURE 7 (*A*) Configuration of alamethicin molecules in a persistent channel proposed by Fox and Richards (1982). Two molecules at opposite sides of the channel are shown with molecular structure based on the x-ray crystallography data of Fox and Richards (1982) in the Brookhaven Data Library. The N-terminals of the molecules are at the top of the diagram. The Gln^7 side chains of the molecules clearly protrude into the channel pore, forming a constriction at the level indicated by the dashed line *aa'*. (*B*) Schematic cross section of the persistent channel pore at its constriction along the plane *aa'* indicated in *A*. This channel is formed by seven alamethicin molecules. The protruding Gln^7 side chains are represented by circles of radius *z*. The centers of the circles are at the corners of the regular heptagon (*dashed line*). A current-conducting ion at closest approach to the protruding Gln^7 side chains is represented by the filled disc of radius *a*. The effective pore area of the channel according to our model is the gray region. r_n^{max} (indicated by the thick scale bar) is the maximum radius of an ion that can pass through the channel.

controlled by the size of the channel pore at the constriction. The spreading resistance R_n^{sp} then effectively includes the resistance of the buffer medium on either side of the constriction. In a cross section of the channel at the level of the channel constriction (*aa'* in Fig. 7 *A*), we represent the protruding Gln^7 side chains as discs with radius *z* and centers at the corners of a regular polygon (Fig. 7 *B*). The number of sides of the polygon is the number of alamethicin molecules forming the channel.

From our experiment data, the equivalent radii r_n^{eq} of the channel pore calculated are not significantly larger than the crystal radius of a typical unhydrated ion (~1 Å; Hille, 1984b). It is inappropriate to regard the electrolyte inside the channel pore as a continuous medium. A systematic way to take into account the finite size of the ions is to represent the ions moving through the channel as spheres with the radius *a* of unhydrated ions. The unhydrated ionic radius is used because an ion passing through the channel pore constriction can be solvated partially by the hydrophilic Gln^7 side chains at the constriction. Ions can approach the channel boundary formed by the Gln^7 side chains as close as their ionic radius, as shown in Fig. 7 *B*. Because of the finite radius of the ions, there is a region in the channel pore that is effectively inaccessible to the ions. The effective conducting area of the channel pore at the constriction is just the area that is accessible to the center of an ion (the gray region in Fig. 7 *B*).

The areas of the gray region in Fig. 7 *B* were fitted to the experimentally derived values of $\pi(r_n^{eq})^2$ by varying the parameters *a*, *z*, and N_1, the number of alamethicin monomers in the state 1 channel. We do not presuppose N_1 because it is possible that there are some lower conductance states that were not properly resolved from the closed state (Hanke and Boheim, 1980). Besides, aggregates containing more than two monomers may still be nonconducting (Spach et al., 1989). All values of N_1 can give an acceptable fit between the calculated areas of the gray region and $\pi(r_n^{eq})^2$, but only $N_1 = 5$ gives a reasonable value of 1.1 Å for *a* comparable to the ionic radius of Na^+ ion (0.95 Å). ($N_1 = 4$ gives $a = 0.5$ Å, whereas $N_1 = 6$ gives $a = 1.7$ Å.) The best value of *z* for $N_1 = 5$ is 2.3 Å (Fig. 8). This agrees reasonably with our model, as the van der Waals radius of the Gln^7 side chains is 2.6 Å for the amide group and 2.1 Å for the carboxyl group (Sutton, 1958).

In Fig. 8, the agreement between the model channel pore area and the value of $\pi(r_n^{eq})^2$ is good for the lower conductance states (up to state 4). Starting from state 5 ($N_n = 9$), the model channel areas are lower than that of $\pi(r_n^{eq})^2$. This deviation may be due to steric hindrance in fitting the alamethicin molecules together in the channel aggregate. Fig. 9 is a schematic diagram showing how, in a channel with a small number of monomers, the protruding Gln side chains can approach one another closely, so that our model

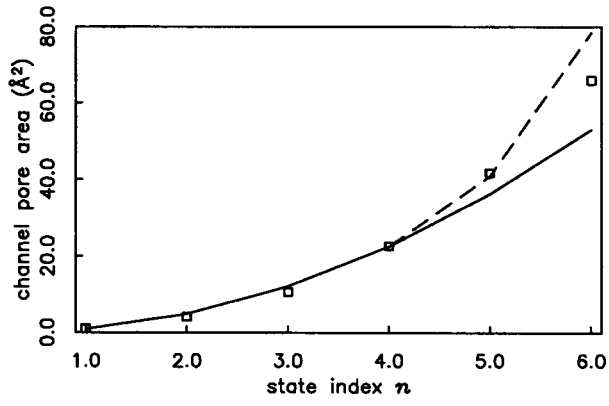

FIGURE 8 Graph of equivalent pore areas $\pi(r_n^{eq})^2$ (*open boxes*) and theoretical pore areas calculated according to our molecular model for various persistent channel conductance states. The solid line is model pore area calculated using $N_1 = 5$, $z = 2.3$ Å and $a = 1.1$ Å, with no helix steric hindrance considered. The dashed line is calculated using the same values for *z* and *a*, but with correction due to steric hindrance of the main helices modeled as discs of radius 5.7 Å, whose centers are 4.3 Å from the centers of the Gln^7 discs (see Fig. 9).

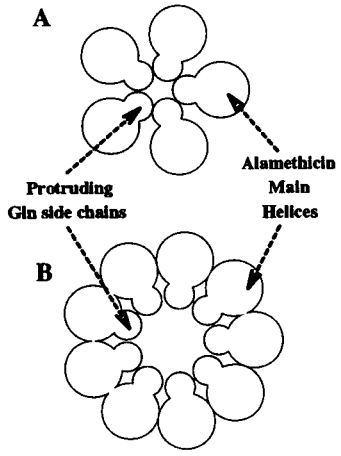

FIGURE 9 Schematic cross sections at the level of the pore constriction of a persistent channel at various conductance states, showing how our modified "barrel-stave" model may not be exact in channels in higher conductance states because of steric hindrance from the main alamethicin helices. (*A*) Channel in conductance state 1 formed by five alamethicin monomers. (*B*) Channel in conductance state 5 formed by nine monomers.

is accurate (Fig. 9 *A*). In channels with more monomers (Fig. 9 *B*), the main helices of the alamethicin monomers prevent the protruding Gln^7 side chains from approaching one another closely. Using the simple model in Fig. 9 and assuming that the steric hindrance only takes effect at $N_n > 8$, the correction due to helix steric hindrance can be estimated. The agreement between the corrected model pore area and $\pi(r_n^{eq})^2$ is better but not exact (Fig. 8), which is to be expected for the crude representation of the complex shape of the main alamethicin helix with a simple disc in our model.

Fig. 10 shows that the effective channel conductance $1/R_n^{ch}$ is directly proportional to the equivalent pore area $\pi(r_n^{eq})^2$ for various persistent channel conductance states:

$$1/R_n^{ch} = K\pi(r_n^{eq})^2, \quad (4)$$

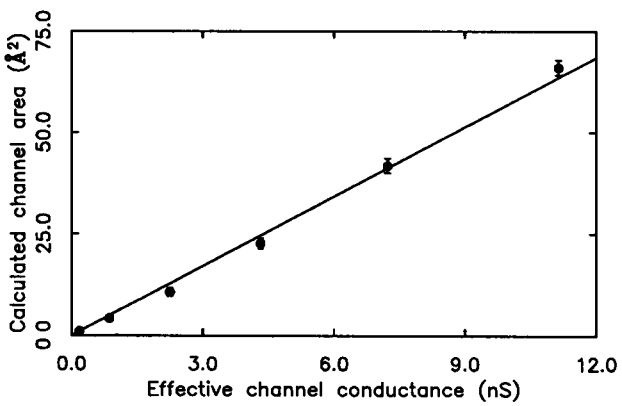

FIGURE 10 Graph of the equivalent pore area $\pi(r_n^{eq})^2$ versus the actual channel conductance $1/R_n^{ch}$ for various persistent channel conductance states. The line is fitted by linear regression.

where K is the slope of the graph. This empirical linear relation implies that the channel energy barrier terms E_n^+ and E_n^- in Eq. 1 do not change significantly as r_n^{eq} changes over an order of magnitude. Whereas the channel constriction for a channel in state 5 or 6 is large enough so that an ion can probably pass through the channel with most of its first shell of water of hydration intact, an ion must shed most of its hydration shell to pass through a channel in state 1 or 2. For the energy barrier experienced by ions crossing the channel to be independent of the channel size, the hydration energy (Edsall and McKenzie, 1978) of the ion must be effectively compensated by the interaction energy of the ion and the polar Gln side chains forming the channel constriction.

The value of K from Fig. 10 is 1.7×10^{10} Sm^{-2}. This gives an effective channel conductance that corresponds to the conductance of a disc of 1 M NaCl buffer at 7°C with area $\pi(r_n^{eq})^2$ and thickness ~3 Å. Although the channel should not be modeled simply as a disc of continuous medium, the estimated thickness of the disc is nevertheless in reasonable agreement with the dimensions of the channel constriction caused by the protruding Gln^7 side chains. The value of the parameter K derived in our model of the alamethicin channel with a constriction is not unrealistic.

In our modeling, we find that the channel in state 1 probably contains five monomers. Using our model, we can calculate that an aggregate with four monomers will form a channel with model pore area of 0.08 $Å^2$. Assuming the empirical relation in Eq. 4, we calculate its conductance to be about 0.012 nS in 1 M NaCl buffer. This conductance value is 1/12 that of our conductance state 1 and is not resolved from the closed conductance state (state 0) in our experiments because of low applied potential and high filtering frequency used in our experiment and the short dwell time of the channel in that state. However, this matches within experimental error the conductance value of the lowest conductance state observed by Hanke and Boheim (1980).

The equivalent radius r_n^{eq} calculated for state 1 is 0.6 Å, substantially smaller than the Na^+ ion radius (0.95 Å). This can be understood with our model. The channel is permeable to ions with radii less than the radius r_n^{max} of the circle inscribed by the protruding Gln^7 side chains surrounding the channel pore (Fig. 7 *B*), which can be much larger than r_n^{eq} (Table 2). For $N_n = 4$, $r_n^{max} = 0.95$ Å, so that it is not permeable to Ca^{2+} ions with ionic radius of 0.99 Å (Hanke and Boheim, 1980). For state 1, r_n^{max} is 1.57 Å, so channels in that state are permeable to ammonium ions with ionic radius of 1.5 Å but not to methylammonium ions with ionic radius of 2.3 Å (Gordon and Haydon, 1975). $(EtOH)NH_3^+$ ions with ionic dimensions of 2.5 Å × 3.0 Å can pass through channels in state 3 with $r_n^{max} = 2.9$ Å but not channels in state 2 with $r_n^{max} = 2.3$ Å (Eisenberg et al., 1977). However, there are cases where ions with radii not significantly larger than r_n^{max} may still pass through the channel (Laüger et al., 1980), like channels in state 2, which are permeable to dimethylammonium ions with radius of

2.6 Å (Gordon and Haydon, 1975). This is because the picture that the alamethicin channel has a fixed pore size ignores the flexibility (Furois-Corbin and Pullman, 1986b) and constant intramolecular and intermolecular thermal motion (Karplus and Petsko, 1990) of alamethicin molecules in the channel. Also, the "hard-sphere" model for ions ignores long-range ion-peptide interaction, which is also important in determining the permeability of the channel to ions. In some cases, ions with radii smaller than r_n^{max} still cannot pass through the channel, probably because of strong interaction between the ions and the peptide side chains (Mueller, 1976; Hall, 1978), like channels in state 4 with r_n^{max} = 3.7 Å, which are impermeable to trimethylammonium ions with radius of 2.8 Å (Gordon and Haydon, 1975).

Although our model is not the only one that can account for the nonohmic behavior of alamethicin channels at high V_{ap} (Lavar, 1994), the configuration of the channel-forming alamethicin monomers assumed in our model is more realistic and is supported by many previous studies. In our model, the hourglass shape of the channel pore implies that the current flux density in the channel vicinity has no abrupt change to generate nonuniform ion concentration in the buffer as assumed by Lavar. Levels of open-channel current noise calculated based on our model agree much better with experimental measurement (forthcoming paper) than those based on Lavar's model.

"Reversed-molecule" model for nonpersistent channels

A simple, plausible model that can qualitatively explain most of the observations in our experiments, including the formation of both persistent and nonpersistent channels by purified alamethicin R_f50, their relative abundance, and the difference in their kinetic behavior and conductance values, is the "reversed-molecule" model. In this model, we assume that one of the alamethicin monomers in the aggregate forming a nonpersistent channel is aligned with its dipole moment antiparallel to the external electric field, whereas the rest of the alamethicin monomers are properly oriented with their dipole moment parallel to the external field.

In the presence of a lipid bilayer, alamethicin molecules can be in three populations: free aqueous alamethicin, adsorbed alamethicin on the bilayer surface with helix axis parallel to the bilayer surface, and inserted alamethicin spanning the bilayer with helix axis normal to the bilayer (Baumann and Mueller, 1974). These three populations are in thermodynamic equilibrium. Under our experimental conditions, in the absence of transmembrane applied potential, there are many more adsorbed than inserted alamethicin molecules (Huang and Wu, 1991).

Unlike alamethicin R_f30, molecules of alamethicin R_f50 are electrically neutral in the pH environment used in our experiment. Therefore, a fraction of the alamethicin molecules adsorbed to the lipid bilayer may form dimers with their helix dipole moments (Hol et al., 1978) in antiparallel alignment to lower their electrostatic energy because the lipid bilayer environment, with its lower dielectric constant (Edmonds, 1985), does not effectively screen the electrostatic interaction between the dipoles. In the dimer configuration, most of the dipole moments of the individual molecules are canceled out because of their antiparallel alignment. However, the irregular shape of the molecules prevents the dipole moments from aligning completely, so that there is a smaller "residual" dimer dipole moment.

A transmembrane applied electric field shifts the equilibrium toward the inserted alamethicin, which, with its dipole aligned parallel to the external field, has a lower electrostatic energy. Because of the smaller "residual" dipole moment of the dimers, they are not as effectively inserted into the bilayer by the applied field. A nonpersistent channel can only form when several inserted alamethicin monomers and one inserted dimer aggregate together. Thus a high applied potential is required to insert the dimers into the lipid bilayer in significant numbers before nonpersistent channels can be observed. In contrast, persistent channels can be generated at a lower applied potential because they are formed entirely from alamethicin monomers that are inserted more effectively by the applied potential into the membrane than the dimers.

Inserted alamethicin molecules must aggregate into channels through attractive interaction. This attraction is probably mediated through the lipid bilayer. Although the dominating interaction between inserted alamethicin monomers may be attractive, to form persistent channels, the electrostatic repulsion between their parallel dipole moments must be overcome to form dimeric and trimeric aggregates before they are stabilized by the shorter-range Lennard-Jones attraction between them (Furois-Corbin and Pullman, 1986a,b). Formation of persistent channels is therefore suppressed by the slow aggregation of the monomers into channels, so that although persistent channels can appear at a lower applied potential, they are much less frequently formed than nonpersistent channels. On the other hand, an inserted dimer with its smaller "residual" dipole moment generates less electrostatic dipole-dipole repulsion against other inserted monomers in the surrounding lipid bilayer and provides a nucleus for aggregate formation. Under the high channel-inducing potential, a large number of properly aligned monomers are available in the lipid bilayer to aggregate around the dimer. Thus, multiple nonpersistent channels were generated rapidly during the channel-inducing voltage pulse in our experiment.

When enough parallel monomers join an aggregate to form a conducting channel pore in persistent channels, the repulsion between their parallel dipole moments is effectively screened by the buffer solution in the channel pore. Energetically favorable interactions between the hydrophilic side chains and water molecules and ions in the channel pore further stabilize the channel. The channel very seldom enters the trimeric or tetrameric nonconducting states in which the parallel, mutually repelling dipoles of the monomers are closely packed. Thus the persistent channels

stayed open for a long time once they were obtained in our experiment.

In the presence of reversed molecules, the nonconducting trimeric or tetrameric aggregates are energetically more favorable than larger aggregates. In a smaller aggregate, the parallel molecules can approach the reversed molecule closely and the electrostatic attraction between their antiparallel dipole moments is not screened by the aqueous channel pore. When the applied potential was reduced in our experiments, the concentration of inserted alamethicin monomers in the lipid bilayer decreased. Parallel molecules left the energetically unfavorable conducting aggregates. Only smaller, nonconducting dimers or trimeric aggregates, each containing a reversed molecule, remained so that the nonpersistent channels disappeared after a short time.

In our experiments and those by Boheim (1974) done under low temperature, mostly nonpersistent channels were observed, whereas at room temperature the persistent channels dominated (Bezrukov and Vodyanoy, 1993). This agrees with the observation by Woolley and Wallace (1993) that low temperature favors association of adsorbed alamethicin in lipid bilayers, so more dimers can form to generate nonpersistent channels at a low temperature. This dimer association is partly mediated through interactions between the alamethicin polypeptides and the lipid bilayer (Huang and Wu, 1991). Large temperature dependence in the properties of the lipid bilayer between 7 and 25°C probably causes the drastic change in the relative abundance of the two classes of channels at different temperatures.

Conversion of persistent to nonpersistent channels is rare because the concentration of inserted dimers is much lower than that of the inserted monomers. Conversion of nonpersistent to persistent channels is also rare because the reversed molecule in the aggregate is more strongly attracted by the other properly aligned molecules because of its antiparallel dipole moment and has little tendency to leave the aggregate.

Nonpersistent channels were not observed in experiments using alamethicin R_f30 samples (Eisenberg et al., 1973; Boheim, 1974), probably because electrostatic repulsion between the negative charges on Glu^{18} of alamethicin R_f30 molecules prevents the formation of dimers in the first place.

In our experiments, the relative frequency of observation of persistent and nonpersistent channels was not significantly affected by whether alamethicin was on just one or both sides of the bilayer. This agrees with our model that the channel-gating mechanism involves an initial voltage-sensitive insertion of alamethicin into the lipid bilayer followed by a rate-limiting aggregation step, as proposed in the original barrel-stave model (Baumann and Mueller, 1974). The monomers needed to form both the persistent and nonpersistent channels are inserted from the side of the bilayer at a higher potential. The applied potential prevents adsorbed monomers from inserting into the bilayer from the other side even if they are present. Thus, the frequency of formation of persistent and nonpersistent channels is unaffected by the presence or absence of alamethicin on the side of the bilayer with a lower potential.

Because the length of the alamethicin molecules in helical form is just enough to span the hydrophobic carbon chain region of the lipid bilayer (Fox and Richards, 1982), the reversed molecule probably spans the bilayer with its terminals at more or less the same level as the other molecules in the channel. Fig. 11 shows that Pro^{14} of the reversed molecule should be at about the same level as Gln^7 of the parallel molecules and facing into the channel pore (Kerr and Sansom, 1993). Thus, the protruding Gln^7 side chains at the channel constriction probably face one of the $-CH_2-$ groups of the Pro^{14} of the reversed molecule. The channel pore areas at the channel constriction can be calculated using our molecular model, with correction allowed for the smaller radius b of the Pro^{14} side chain from the reversed molecule. The equivalent pore area $\pi(r_n^{eq})^2$ of the nonpersistent conductance states can be calculated from the experimentally determined channel conductance by applying the empirical relation Eq. 4 to nonpersistent channels. The model pore area can be fitted to $\pi(r_n^{eq})^2$ by varying the value of b. The best value of b is found to be 2.0 Å (Fig. 12), which agrees well with the van der Waals radius of 2.1 Å for the Pro^{14} $-CH_2-$ group (Sutton, 1958).

According to our model, conversion from nonpersistent to persistent channels without channel closing can occur when the antiparallel monomer in the channel aggregate flip-flops 180° into a parallel orientation while remaining a part of the channel aggregate. The rarity of such conversions in our experiments makes it highly unlikely that a monomer flipping from antiparallel to parallel orientation can occur frequently enough to be the mechanism generating channel conductance state transitions, as proposed in the flip-flop model (Boheim et al., 1983). Our experimental observations, especially the types of possible transitions between odd and normal conductance states in unpurified alamethicin R_f30 samples, support the conductance state transition mechanism proposed in the barrel-stave model (Baumann and Mueller, 1974).

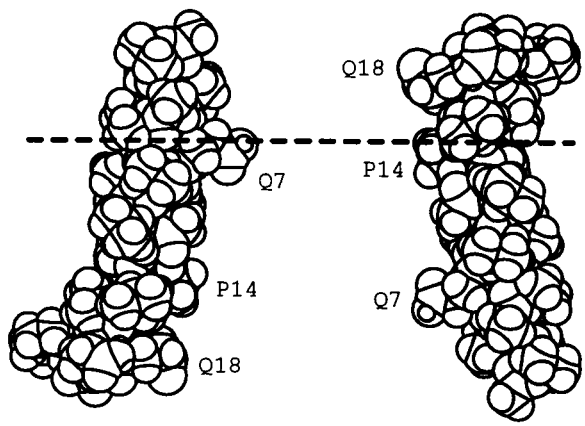

FIGURE 11 Diagram showing two antiparallel alamethicin molecules with terminals at the same level. Note that Gln^7 (Q7) of one molecule is at the same level as Pro^{14} (P14) of the other.

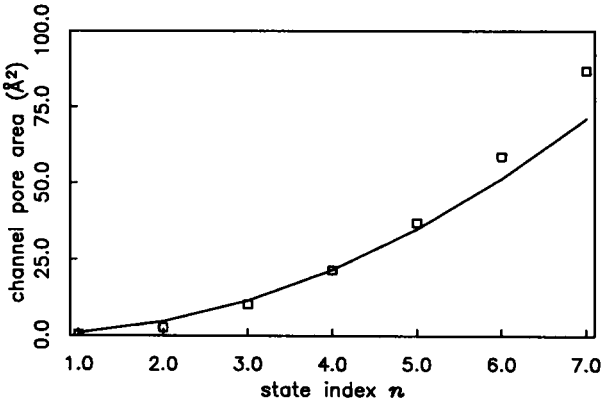

FIGURE 12 The graph of equivalent pore areas $\pi(r_n^{eq})^2$ (*open boxes*) and the best-fitted theoretical pore areas (*solid line*) calculated from the "reversed-molecule" model.

CONCLUSION

Our studies of alamethicin channel current using patch-clamp techniques reveals that alamethicin polypeptides can form two distinct classes of channels: persistent channels that have a long lifetime (minutes to hours) and the non-persistent channels that last a short time (<1 min). Each of the two classes of channels has a distinctive set of conductance states. Comparing the electrical and kinetic properties of the two classes of channels we observed with results of previous studies (Eisenberg et al., 1973; Boheim, 1974; Bezrukov and Vodyanoy, 1993) shows that alamethicin R_f50 forms mostly nonpersistent channels at low temperatures (3–7°C), whereas persistent channels are formed by alamethicin R_f30 at all temperatures as well as by alamethicin R_f50 at room temperature.

Considering the results of studies on the secondary structure and aggregate configuration of alamethicin, we proposed a molecular model for the persistent channels based on the crystalline secondary structure of alamethicin molecules (Fox and Richards, 1982). According to this modified barrel-stave model, the aqueous pore of the persistent channel surrounded by parallel alamethicin monomers has a constriction generated by Gln^7 side chains protruding from the main alamethicin helices into the channel pore. This constriction provides the energy barrier that, according to a theory proposed by Laüger (1975), generates the nonohmic current in alamethicin channels observed under high applied potential (Eisenberg et al., 1973; Taylor and de Levie, 1991). By considering the conducting ions as "hard spheres" with a finite radius, the conductance values of the persistent channels in various conductance states can be calculated from the model, and many previously published ion permeability experiment results can be quantitatively accounted for.

The existence, relative abundance at various temperatures, and kinetic properties of the nonpersistent channels observed in our experiments can be explained qualitatively by our reversed-molecule model in which the nonpersistent alamethicin channels differ from persistent channels by having one of the alamethicin monomers in the channel-forming aggregate oriented antiparallel to the others. According to this model, the observed kinetic properties of the two classes of alamethicin channels support the mechanisms for voltage-dependent channel gating proposed in the original barrel-stave model (Baumann and Mueller, 1974), in which the voltage-dependent insertion of alamethicin molecules into the lipid bilayer precedes the aggregation of the inserted molecules to form channels.

We would like to thank T. Saido for pioneering work on alamethicin in artificial bilayers, L. R. Opsahl for useful discussions, S.-L. Chan for help in generating the molecular diagrams, and J. K. Foskett for help and support in the preparation of the manuscript.

This work was supported by a grant from the Office for Naval Research (N00014-89J-1656) and by facilities of the Developmental Resource for Biophysical Imaging and Optoelectronics provided by the National Institutes of Health (P41-RR04224) and the National Science Foundation (DIR 8800278).

REFERENCES

Archer, S. J., J. F. Ellena, and D. S. Cafiso. 1991. Dynamics and aggregation of the peptide ion channel alamethicin. *Biophys. J.* 60:389–398.

Balasubramanian, T. M., N. C. E. Kendrick, M. Taylor, G. R. Marshall, J. E. Hall, I. Vodyanoy, and F. Reusser. 1981. Synthesis and characterization of the major component of alamethicin. *J. Am. Chem. Soc.* 103:6127–6132.

Banerjee, U., F.-P. Tsui, T. N. Balasubramanian, G. R. Marshall, and S. I. Chan. 1983. Structure of alamethicin in solution: one- and two-dimensional ^1H NMR studies at 500 MHz. *J. Mol. Biol.* 165:757–775.

Baumann, G., and P. Mueller. 1974. A molecular model of membrane excitability. *J. Supramol. Struct.* 2:538–557.

Bezrukov, S. M., and I. Vodyanoy. 1993. Probing alamethicin channels with water-soluble polymers. *Biophys. J.* 64:16–25.

Boheim, G. 1974. Statistical analysis of alamethicin channels in black lipid membranes. *J. Membr. Biol.* 19:277–303.

Boheim, G., S. Gelfert, G. Jung, and G. Menestrina. 1987. α-Helical ion channels reconstituted into planar bilayers. *In* Ion Transport Through Membranes. K. Yagi and B. Pullman, editors. Academic Press, New York. 131–145.

Boheim, G., W. Hanke, and G. Jung. 1983. Alamethicin pore formation: voltage-dependent flip-flop of α-helix dipoles. *Biophys. Struct. Mech.* 9:181–191.

Boheim, G., and H.-A. Kolb. 1978. Analysis of the multi-pore system of alamethicin in a lipid membrane I. *J. Membr. Biol.* 38:99–150.

Bosch, R., G. Jung, H. Schmitt, and W. Winter. 1985. Crystal structure of Boc-Leu-Aib-Pro-Val-Aib-Aib-Glu(Obzl)-Glu-Phl × H_2O, the C-terminal nonapeptide of the voltage-dependent ionophore alamethicin. *Biopolymers.* 24:979–999.

Brumfeld, V., and I. R. Miller. 1989. Electric field dependence of alamethicin channels. *Biochim. Biophys. Acta.* 1024:49–53.

Burgess, A. W., and S. J. Leach. 1973. An obligatory α-helical amino acid residue. *Biopolymers.* 12:2599–2605.

Butters, T., P. Hütter, G. Jung, N. Pauls, H. Schmitt, G. M. Sheldrick, and W. Winter. 1981. On the structure of the helical *N*-terminus in alamethicin—α-helix or 3_{10}-helix. *Angew. Chem. Int. Ed. Engl.* 20:889–890.

Cahalan, M., and E. Neher. 1992. Patch clamp techniques: an overview. *Methods Enzymol.* 207:3–14.

Cascio, M., and B. A. Wallace. 1988. Conformation of alamethicin in phospholipid vesicles: implications for insertion models. *Proteins Struct. Funct. Genet.* 4:89–98.

Chandrasekhar, K., M. K. Das, A. Kumar, and P. Balaram. 1988. Molecular conformation of alamethicin in dimethylsulfoxide solution. *Int. J. Pept. Protein Res.* 32:167–174.

Cherry, R. J., D. Chapman, and D. E. Graham. 1972. Studies of the conductance changes induced in bimolecular lipid membranes by alamethicin. *J. Membr. Biol.* 7:325–344.

Coronado, R. 1985. Effect of divalent cations on the assembly of neutral and charged phospholipid bilayers in patch-recording pipettes. *Biophys. J.* 47:851–857.

Coronado, R., and R. Latorre. 1983. Phospholipid bilayers made from monolayers on patch-clamp pipettes. *Biophys. J.* 43:231–236.

Davis, D. G., and B. F. Gisin. 1981. 600 MHz proton magnetic resonance studies of natural and synthetic alamethicin. *FEBS Lett.* 133:247–251.

Edmonds, D. T. 1985. The α-helix dipole in membranes: a new gating mechanism for ion channels. *Eur. Biophys. J.* 13:31–35.

Edsall, J. T., and H. A. McKenzie. 1978. Water and proteins. I. The significance and structure of water: its interaction with electrolytes and non-electrolytes. *Adv. Biophys.* 10:137–207.

Eisenberg, M., J. E. Hall, and C. A. Mead. 1973. The nature of the voltage-dependent conductance induced by alamethicin in black lipid membranes. *J. Membr. Biol.* 14:143–176.

Eisenberg, M., M. E. Kleinberg, and J. H. Shaper. 1977. Channels across black lipic membranes. *Ann. N.Y. Acad. Sci.* 303:281–291.

Esposito, G., J. A. Carver, J. Boyd, and I. D. Campbell. 1987. High-resolution ^{1}H NMR study of the solution structure of alamethicin. *Biochemistry.* 26:1043–1050.

Fleischmann, M., C. Gabrielli, and M. T. G. Labram. 1983. Analysis of the voltage-gated alamethicin induced channel conductance in lipid bilayers as a triggered birth and death stochastic process. *In* Physical Chemistry of Transmembrane Ion Motions. G. Spach, editor. Elsevier, Amsterdam, Oxford, New York. 367–374.

Fox, R. O., Jr., and F. M. Richards. 1982. A voltage-gated ion channel model inferred from the crystal structure of alamethicin at 1.5 Å resolution. *Nature.* 300:325–330.

Fraternali, F. 1990. Restrained and unrestrained molecular dynamics simulations in the *NVT* ensemble of alamethicin. *Biopolymers.* 30: 1083–1099.

Furois-Corbin, S., and A. Pullman. 1986a. Theoretical study of the packing of α-helices by energy minimization: effect of the length of the helices on the packing energy and on the optimal configuration of a pair. *Chem. Phys. Lett.* 123:305–310.

Furois-Corbin, S., and A. Pullman. 1986b. Theoretical study of the packing of α-helices of poly(L-alanine) into transmembrane bundles. Possible significance for ion-transfer. *Biochim. Biophys. Acta.* 860:165–177.

Furois-Corbin, S., and A. Pullman. 1988. Conformation and pairing properties of the n-terminal fragments of trichorzianine and alamethicin: a theoretical study. *Biochim. Biophys. Acta.* 944:399–413.

Gisin, B. F., S. Kobayashi, D. G. Davis, and J. E. Hall. 1977. Synthesis of biologically active alamethicin. *In* Peptides: Proceedings of the Fifth American Peptide Symposium. M. Goodman and J. Meienhofer, editors. John Wiley and Sons, New York, Chichester, Brisbane, Toronto. 215–217.

Gordon, L. G. M., and D. A. Haydon. 1972. The unit conductance channel of alamethicin. *Biochim. Biophys. Acta.* 255:1014–1018.

Gordon, L. G. M., and D. A. Haydon. 1975. Potential-dependent conductances in lipid membranes containing alamethicin. *Phil. Trans. R. Soc. Lond.* B270:433–447.

Gordon, L. G. M., and D. A. Haydon. 1976. Kinetics and stability of alamethicin conducting channels in lipid bilayers. *Biochim. Biophys. Acta.* 436:541–556.

Hall, J. E. 1975. Toward a molecular understanding of excitability. *Biophys. J.* 15:934–939.

Hall, J. E. 1978. Channels in black lipid films. *In* Membrane Transport in Biology I: Concepts and Models. Springer-Verlag, Berlin, Heidelberg, New York. 475–531.

Hall, J. E., and I. Vodyanoy. 1984. Alamethicin, a rich model for channel behaviour. *Biophys. J.* 45:233–247.

Hamill, O. P., A. Marty, E. Neher, B. Sakmann, and F. J. Sigworth. 1981. Improved patch-clamp techniques for high-resolution current recording from cells and cell-free membrane patches. *Pflüegers Arch. Eur. J. Physiol.* 391:85–100.

Hanke, W., and G. Boheim. 1980. The lowest conductance state of the alamethicin pore. *Biochim. Biophys. Acta.* 596:456–462.

Hanke, W., C. Mithfessel, U. Wilmsen, and G. Boheim. 1984. Ion channel reconstitution into lipid bilayer membranes on glass patch pipettes. *Bioelectrochem. Bioenergetics.* 12:329–339.

Haris, P. I., and D. Chapman. 1988. Fourier transform infrared spectra of the polypeptide alamethicin and a possible structural similarity with bacteriorhodopsin. *Biochim. Biophys. Acta.* 943:375–380.

Hille, B. 1984a. Ionic Channels of Excitable Membranes. Sinauer Associates, Sunderland, MA. 184–186.

Hille, B. 1984b. Ionic Channels of Excitable Membranes. Sinauer Associates, Sunderland, MA. 163–168.

Hol, W. G. J., P. T. van Duijnen, and H. J. C. Berendsen. 1978. The α-helix dipole and the properties of proteins. *Nature.* 273:443–446.

Holm, R. 1967. Electric Contacts: Theory and Application. Springer-Verlag, Berlin, New York. 9–20.

Huang, H. W., and Y. Wu. 1991. Lipid-alamethicin interactions influence alamethicin orientation. *Biophys. J.* 60:1079–1087.

Jung, G., and N. Dubischar. 1975. Conformational changes of alamethicin induced by solvent and temperature. *Eur. J. Biochem.* 54:395–409.

Karplus, M., and G. A. Petsko. 1990. Molecular dynamics simulations in biology. *Nature.* 347:631–638.

Kelsh, L. P., J. F. Ellena, and D. S. Cafiso. 1992. Determination of the molecular dynamics of alamethicin using ^{13}C NMR: implications for the mechanism of gating of a voltage-dependent channel. *Biochemistry.* 31:5136–5144.

Kerr, I. D., and M. S. P. Sansom. 1993. Hydeophilic surface maps of channel-forming peptides: analysis of amphipathic helices. *Eur. Biophys. J.* 22:269–277.

Latorre, R., and O. Alvarez. 1981. Voltage-dependent channels in planar lipid bilayer membranes. *Physiol. Rev.* 61:77–150.

Laüger, P. 1975. Shot noise in ion channels. *Biochim. Biophys. Acta.* 413:1–10.

Laüger, P., W. Stephan, and E. Frehland. 1980. Fluctuations of barrier structure in ionic channels. *Biochim. Biophys. Acta.* 602:167–180.

Lavar, D. R. 1994. The barrel-stave model as applied to alamethicin and its analogs reevaluated. *Biophys. J.* 66:355–359.

Marshall, G. R., and T. M. Balasubramanian. 1979. Alamethicin: purification, characterization, conformational and synthetic studies. *In* Peptide Structure and Biological Function: Proceedings of the Sixth American Peptide Symposium. E. Gross and J. Meienhofer, editors. Pierce Chemical Company, Rockford, IL. 639–646.

Marshall, G. R., E. E. Hodgkin, D. A. Langs, G. D. Smith, J. Zabrocki, and M. T. Leplawy. 1990. Factors governing helical preference of peptides containing multiple α, α-dialkyl amino acids. *Proc. Natl. Acad. Sci. USA.* 87:487–491.

Martin, D. R., and R. J. P. Williams. 1975. The nature and function of alamethicin. *Biochem. Soc. Trans.* 3:166–167.

Mathew, M. K., and P. Balaram. 1983a. Alamethicin and related membrane channel forming polypeptides. *Mol. Cell. Biochem.* 50:47–64.

Mathew, M. K., and P. Balaram. 1983b. A helix dipole model for alamethicin and related transmembrane channels. *FEBS Lett.* 157:1–5.

Maxwell, J. C. 1873. A Treatise on Electricity, and Magnetism. Clarendon Press, Oxford. 426–434.

Mueller, P. 1976. Molecular aspects of electrical excitation in lipid bilayers and cell membranes. *Horizons Biochem. Biophys.* 2:230–284.

Mueller, P., and D. O. Rudin. 1968. Action potentials induced in biomolecular lipid membranes. *Nature.* 217:713–719.

North, C. L., J. C. Franklin, R. G. Bryant, and D. S. Cafiso. 1994. Molecular flexibility demonstrated by paramagnetic enhancements of nuclear relaxation. Application to alamethicin: a voltage-gated peptide channel. *Biophys. J.* 67:1861–1866.

Paterson, Y., S. M. Rumsey, E. Benedetti, G. Némethy, and H. A. Scheraga. 1981. Sensitivity of polypeptide conformation to geometry. Theoretical conformational analysis of oligomers of α-aminoisobutyric acid. *J. Am. Chem. Soc.* 103:2947–2955.

Rinehart, K. L., Jr., J. C. Cook, Jr., H. Meng, K. L. Olson, and R. C. Pandey. 1977. Mass spectrometric determination of molecular formulas for membrane-modifying antibiotics. *Nature.* 27:832–833.

Rizzo, V., S. Stankowski, and G. Schwarz. 1987. Alamethicin incorporation in lipid bilayers: a thermodynamic study. *Biochemistry.* 26: 2751–2759.

Sakmann, B., and G. Boheim. 1979. Alamethicin-induced single channel conductance fluctuations in biological membranes. *Nature.* 282:336–339.

Sansom, M. S. P. 1991. The biophysics of peptide models of ion channels. *Prog. Biophys. Mol. Biol.* 55:139–235.

Sansom, M. S. P. 1993. Alamethicin and related peptaibols—model ion channels. *Eur. Biophys. J.* 22:105–124.

Schmitt, H., and G. Jung. 1985. ^{13}C NMR spectroscopic control of the synthesis of alamethicin F30 and its segments. *Leibigs Ann. Chem.* 1985:345–364.

Smythe, W. R. 1967. Static and Dynamic Electricity. McGraw-Hill, New York. 109–112.

Spach, G., H. Duclohier, G. Molle, and J.-M. Valleton. 1989. Structure and supramolecular architecture of membrane channel-forming peptides. *Biochimie.* 71:11–21.

Stankowski, S., U. Schwarz, and G. Schwarz. 1988. Voltage-dependent pore activity of the peptide alamethicin correlated with incorporation in the membrane: salt and cholesterol effects. *Biochim. Biophys. Acta.* 941:11–18.

Sutton, L. E., editor. 1958. Tables of Interatomic Distances and Configuration in Molecules and Ions. The Chemical Society, London.

Taylor, R. J., and R. de Levie. 1991. "Reversed" alamethicin conductance in lipid bilayers. *Biophys. J.* 59:873–879.

Vogel, H. 1987. Comparison of the conformation and orientation of alamethicin and melittin in lipid membranes. *Biochemistry.* 26: 4562–4572.

Vogel, H. N. L., R. Rigler, S. Meder, G. Boheim, H.-H. Beck, W. Kurth, and G. Jung. 1993. Structural fluctuations between two conformational states of a transmembrane helical peptide are related to its channel-forming properties in planar lipid membranes. *Eur. J. Biochem.* 212: 305–313.

Washburn, E. W., editor. 1929. International Critical Tables of Numerical Data, Physics, Chemistry and Technology, Vol. 6. McGraw-Hill, New York and London. 233–234.

Woolley, G. A., and B. A. Wallace. 1992. Model ion channels: gramicidin and alamethicin. *J. Membr. Biol.* 129:109–136.

Woolley, G. A., and B. A. Wallace. 1993. Temperature dependence of the interaction of alamethicin helices in membranes. *Biochemistry.* 32: 9819–9825.

Yee, A. A., and D. J. O'Neil. 1992. Uniform ^{15}N labeling of a fungal peptide: the structure and dynamics of an alamethicin by ^{15}N amd ^{1}H NMR spectroscopy. *Biochemistry.* 31:3135–3143.